Evaluating detector requirements for the next UV/O/IR flagship observatory

Lazar Buntic[a], Donald F. Figer[a], and Justin P. Gallagher[a]

[a]Rochester Institute of Technology, Center for Detectors, 74 Lomb Memorial Drive, Rochester, NY, USA

ABSTRACT

The next UV/O/IR flagship observatory mission recommended by the 2020 Decadal Survey on Astronomy and Astrophysics requires detector performance beyond what many devices deliver; i.e., lower dark current, lower read noise, higher QE, photon counting capability, etc. We evaluate how detector performance parameters affect the ability of an instrument to satisfy the science goals described in the LUVOIR concept study. We compare the requirements to performance in relevant metrics for current state-of-the-art devices. Current UV/O devices (specifically photon-counting CMOS ones) already perform at a level that meet most of the requirements of the upcoming flagship mission. We find that CMOS devices provide performance characteristics that exceed the requirements and exist in formats that demonstrate scalability beyond tens of mega-pixels. EMCCDs have demonstrated scalability to this size as well, though the excess noise factor introduced by the gain mechanism presents significant issues. MKIDs can resolve photon energy, but have yet to demonstrate scalability to mega-pixel formats. SNSPDs do not currently have readout architectures beyond the kilo-pixel level.

Keywords: LUVOIR, HabEx, decadal, photon counting, single photon, QIS, MKID, CMOS, SNSPD

1. INTRODUCTION

The 2020 Decadal Survey on Astronomy and Astrophysics[1] recommends the next generation flagship observatory as a cross between the architecture of LUVOIR-B (segmented 8-meter UV/O/IR telescope) and HabEx (monolithic 4-meter UV/O/IR telescope), resulting in a 6-meter UV/O/IR space telescope that can fulfill the major goals of both missions. The LUVOIR Final Report and Appendices[2,3] lists a number of science cases and goals, as well as a baseline detector that provides the required level of performance to achieve these goals in the time allotted for the mission.[3] This paper provides an independent calculation of the time required to achieve the science goals for key science missions using the performance parameters of modern photon-counting CMOS devices, whose increased performance can significantly relax the technical constraints on the rest of the observatory and decrease the time required to perform challenging observations. The Decadal Survey states that prior to commencing mission formulation for this UV/O/IR flagship, the Great Observatories Mission and Technology Maturation Program (GOMTMP) must be completed. This paper informs the decisions of mission planners, system integrators, instrument developers, and detector development groups to better prepare for the GOMTMP and have devices appropriate for the maturation program, which will fund development of key detector technologies beyond TRL 5.[1]

The purpose of this paper is to quantitatively describe how the science goals of the UV/O/IR observatory put limitations on the detector performance with regards to the most important parameters. It is not meant to provide strict detector requirements for the candidate detectors for the UV/O/IR flagship. Section 2 describes the science goals of the LUVOIR concept that put the most stringent constraints on detector performance. Section 3 demonstrates how certain detector parameters affect the ability of the telescope to perform the required observations. Section 4 is a brief overview of existing detector technologies, their current state, and how they compare to one another.

Further author information: (Send correspondence to Lazar Buntic)
Lazar Buntic: E-mail: lb4525@rit.edu, Telephone: 814-923-1521

2. LUVOIR SCIENCE GOALS

The Large UltraViolet, Optical, and InfraRed surveyor (LUVOIR) was proposed as the next UV/O/IR great observatory, set to launch in the mid 2030s. The LUVOIR Final Report describes science objectives that would not be possible without the extraordinary pointing stability of the telescope combined with state-of-the-art detector performance. The report presents two major architectures: LUVOIR-A, a telescope with a 15 meter mirror array, and LUVOIR-B, an 8 meter version. While most of the general science goals of the observatory are achievable with either architecture, the LUVOIR report presents some cases that are believed to not be possible (for LUVOIR-B) with the detector technology baselined in the Final Report.[2] We will show in this paper that a sufficiently low-noise detector could save enough time on observations for even the decadal-recommended (6 meter LUVOIR-B analog) architecture to achieve performance capable of these challenging observations.

We use Science Cases (SC) #5, #11 and Additional Case (AC) #6 in the LUVOIR Final Report and Appendices to demonstrate some of the constraints that LUVOIR observations place on detector requirements. These are used to evaluate the performance of low-noise detectors that could be used for the LUVOIR-B High Definition Imager (HDI-B) Ultra-violet/Visible (UVIS) focal plane array as well as the LUVOIR-B LUMOS UVIS detector. These science cases were chosen because each presents a different limiting case: SC#5 used astrometry of bright stars to detect exoplanet masses (with light suppression), and SC#11 planned observations of extremely faint stars in galaxies at intermediate ($z = 1 - 2$) redshift.

Science Case #5 was contingent on the ability of the HDI detector to observe bright objects without saturation, which requires either high full well depth, fast readout, or some balance of the two. The goal of SC#5 was to use the HDI to perform high precision astrometry to measure the orbits and masses of planets of $\sim$54 systems chosen by the exoEarth search performed for SC#1 (as set forth by the LUVOIR Final Report). The goal here is to take two sequences of images: the first to achieve Signal-to-Noise Ratio (SNR)$\sim$25 for the central star ($m_V \approx 4 - 7$) with either an ultra-narrow band filter ($R \approx 9128$) or a broadband filter with a 10-magnitude neutral density filter. The second series of images would serve to obtain the same SNR as the first, but for the reference field stars ($m_V \geq 10$).

SC#11 would have used the HDI to observe very dim ($m_V = 30 - 35$) solar analogs, which one intuitively might expect to be limited by the dark current and read noise of the detector. We show in this paper that due to the background-limited nature of these observations, a large reduction in read noise (RN) turns out to be most effective when the bandpass of observations is narrow (*i.e.* when R is large). This is most evident in observations like those for AC#6, which would have taken low-medium resolution (R$\leq 30,000$) spectra of relatively bright ($m_V \leq 22$) comets, minor planets, and belt objects in the solar system.

For all calculations in this document, we use simple models of the 6-meter telescope architecture recommended for the UV/O/IR observatory in the 2020 Decadal Survey (the 6 meter LUVOIR-B analog), and provide a brief comparison to a similar instrument with improved dark current and read noise.

3. EVALUATING DETECTOR REQUIREMENTS

The LUVOIR concept study team derived the observation times to achieve science goals for the LUVOIR mission by using a set of generic detector parameters that were considered adequate at the time the LUVOIR Final Report was written. LUVOIR's HDI instrument was designed with two primary detectors, one for UVIS bandpasses and the other for NIR.[3] Table 1 contains some of the relevant detector parameters for the UVIS detector of the original HDI-B architecture.

The concept study team chose the pixel size for the HDI-B UVIS detector to provide diffraction limited Nyquist sampling at 500 nm, with an f/26 design, 208 meter focal length, and an 8 meter aperture. Since the specific parameters for the decadal-recommended UV/O/IR Great Observatory won't be decided until the GOMTMP is well underway, the detector to be used on it does not need 6.5 μm pixels so long as the overall design still provides diffraction limited Nyquist sampling at 500 nm.

The team at the Center for Detectors at RIT collaborated with Bob Woodruff to create a tentative design for a "LUVOIR-like" space telescope (henceforth the "GigaCam Instrument") based on a giga-pixel format photon-counting CMOS detector. Figure 1 shows the ray-traces for the GigaCam telescope, where the instrument

is notionally represented by the focal plane. This design utilizes a lower f/# (than LUVOIR) which reduces the overall focal length and could significantly reduce the final size (and therefore cost) of the telescope. The detector for this design is based on current state-of-the-art CMOS photon counting detectors, specifically the Quanta Image Sensor (QIS) design by Gigajot Technology Inc. (Gigajot). The dark current value for the GigaCam instrument is scaled up by a factor of four for 2.2μm pixels from a reported value of 0.0003 e^-/s/pix for 1.1μm pixels in a similar device. This dark current value is an average of the array of an early QIS device, and the read noise is representative of a 65th percentile pixel in terms of performance.[4] We assume a full-system efficiency of 0.21 for the V-band (for HDI-B and Gigacam) for all calculations in this document as this was the reported system efficiency for the full LUVOIR system including the HDI instrument. This includes the primary, secondary, and tertiary mirrors, the fold mirrors, the UVIS/NIR splitter/dichroic, and the detector itself. The reflection and transmission coefficients for these components were not provided independently. An analysis based on varying QE was not performed for this paper. The total integration times presented in the figures in this paper are are not equal to those presented in the LUVOIR Final Report, as there are a number of factors that are not made explicit in the LUVOIR Final Report and assumptions had to be made where information was lacking. Additionally, the calculations in this document use a 6 meter aperture, while LUVOIR-B's was 8 meters.

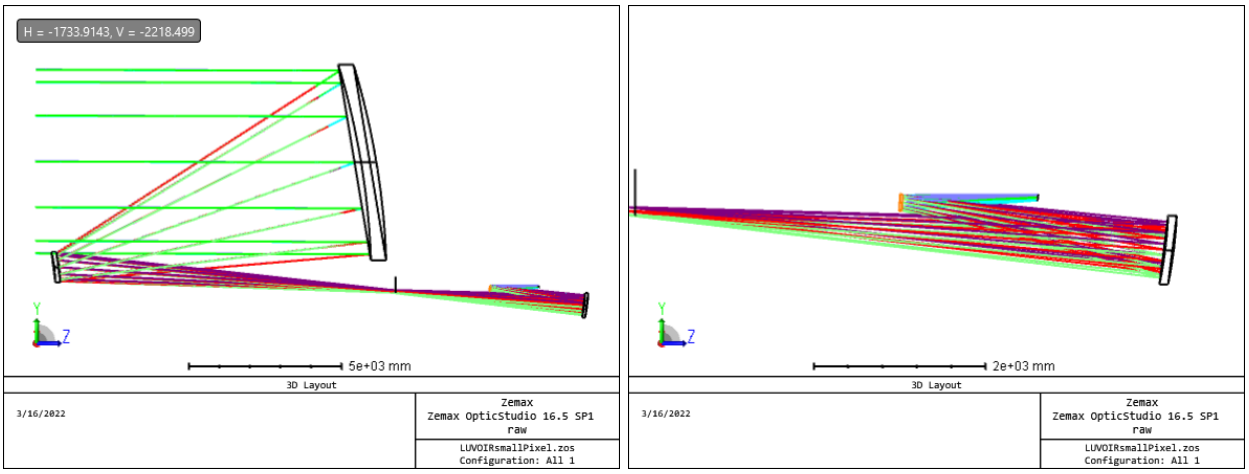

Figure 1. This figure shows ray-traces for the 3 mirror anastigmat of the GigaCam instrument designed by Bob Woodruff.

3.1 Observations of Dim Galaxies

One of the primary goals of the future UV/O/IR flagship is to explore galactic evolution on spatial scales of ∼100 parsec (corresponding to the sizes of large star-forming regions) at high redshift. While the most challenging observations for dwarf galaxies at $z \geq 7$ will be done in the NIR, the LUVOIR report presented a plan to survey $z = 1 - 2$ galaxies for solar analogs in the V-band to map the Main-Sequence Turn-Off (MSTO).[2,3] This survey would entail collecting observations of solar analogs with V-band magnitudes $m_V = 30 - 35$ in order to adequately map the MSTO and the interior morphology of the target galaxies, as well as estimate their age. LUVOIR-B observations were planned to be a series of co-added exposures, with integration times for single frames not exceeding 1200 seconds. The decision to limit single frames to 1200 seconds was not justified in the LUVOIR report beyond the desire to perform cosmic ray removal in the longest observations. It should be noted that each readout incurs read noise, so for the longest exposures the read noise is compounded many times.

Given the weak signal of dim stars, broadband observations quickly become background limited. Observations made with higher spectral resolution also become background limited, but to a lesser degree than broadband observations (*i.e.* reducing the RN of the detector has a larger effect on the time required to achieve the desired SNR when R is large). Figure 2 shows how the integration time is reduced when the RN of the 6 meter LUVOIR-B detector is reduced from 2.5 e^- to 0.25 e^-. The plot on the left shows the time savings as a percentage of the total observing time, while the plot on the right shows the time saved in hours, as well as the total observing time. Although the time reduction for HDI grism spectroscopy (R=500) is less than 7% for $m_V \leq 24$, large

Table 1. The table below shows detector parameters for the HDI-B and GigaCam instruments. Note that the LUVOIR analog recommended in the 2020 Decadal Survey has a mirror diameter of 6 meters.

Parameter	**Unit**	**HDI-B UVIS**	**GigaCam Instrument**
Aperture Diameter	m	8	6
f/#	-	26	9
Focal Length	m	208	54.35
Detector Type	-	CMOS	CMOS
Pixel Size	μm	6.5	2.2
Detector Format	pixels	8192×8192	31.6K × 31.6K
Array Tiling	detectors	3×2	1 × 1
Total Pixels	Gpix	0.40	0.998
Detector Temperature	K	170	204[4]
Read Noise	e^-	2.5	0.21[4]
Dark Current	e^-/s	0.002	0.0012
System QE	-	0.21	0.21

time savings can be achieved in cases where the resolution factor is significantly higher even when the stars are relatively bright.

One of the additional science goals in the LUVOIR Final Report was to perform low-medium resolution ($R \leq 30000$) spectroscopy of minor planets, comets, trans-Neptunian objects, and belt asteroids to $m_V = 22$. Figure 3 shows the total integration times to achieve SNR≥10 with low-medium resolution spectroscopy with HDI-B (R=500) on the left and the LUVOIR-B LUMOS (R=28000) instrument on the right. Although the time savings are minimal for the HDI case ($\approx 1.23\%$), the relatively high R for the LUMOS instrument increases the time savings to $\approx 35.3\%$.

3.2 Observations of Bright Objects

The high fluxes of bright stars present an observational challenge since there is a balance to be struck between the full well depth (FWD) of the detector pixels and the speed at which the device must be read out to avoid saturating those pixels. At a constant flux, a smaller FWD implies that a pixel must be read out more often to avoid saturation. Figure 4 is a simple depiction of this relationship: in order to sustain a certain electron flux at the pixel without saturation, the detector chip must have a certain FWD and frame-rate. The vertical red line represents a frame-rate of 60 frames-per-second, and the horizontal lines trace where it intersects with the three brightest fluxes.

The requirements on the readout rate/frame rate of the device that will be used on the UV/O/IR flagship must also carefully balance power usage and data output volume. A detector with a small FWD saturates faster and must be read out more often, and thus implicitly uses more power, emits more thermal waste, and requires the supporting electronics to handle significantly higher data output volume. It is easy to say that the solution to this issue is to just make detector pixels with higher FWD, but this carries a number of challenges that must be considered by the detector engineers. In some cases, it is not possible to increase the FWD significantly without sacrificing performance in some other metric, such a read noise or dark current.

3.3 Determining Pixel Pitch

Deriving the pixel pitch is done by finding a balance between the resolution limits of the detector and the diffraction cutoff of the optics. Traditionally, we can define a factor Q, which compares the two resolution limits. The Nyquist frequency is defined as

$$\xi_N = \frac{1}{2p}, \tag{1}$$

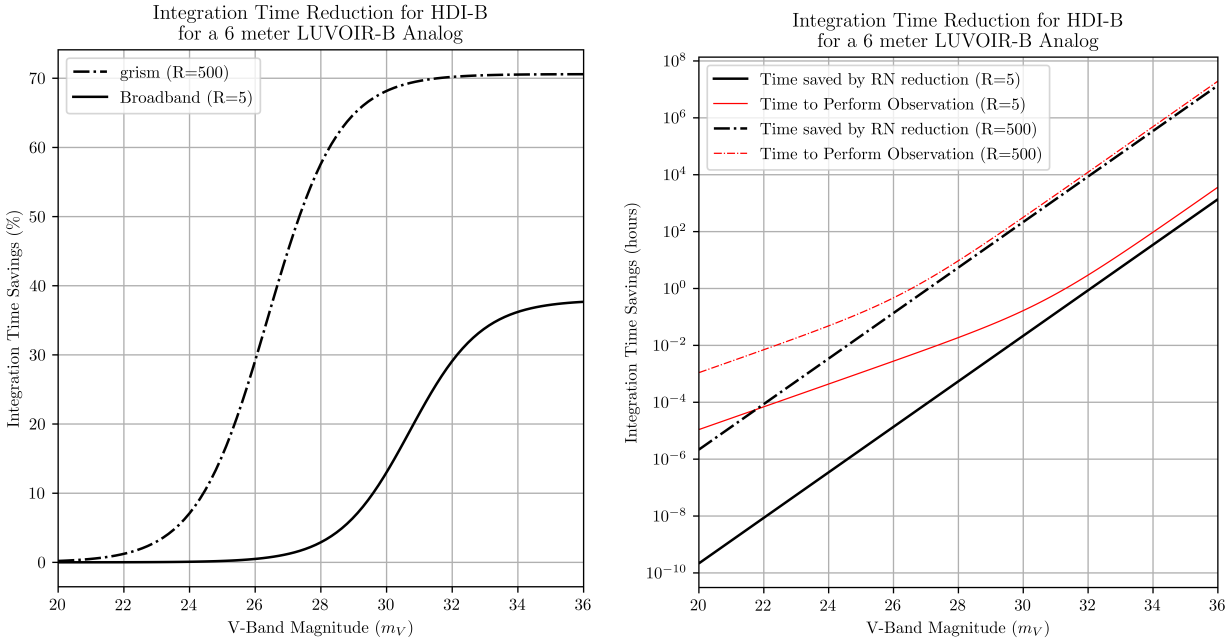

Figure 2. The plot on the left shows the integration time reduction that can be achieved for the HDI-B analog (as a percentage of the total observation time) for stars of $m_V = 20 - 36$ when the RN of the detector is reduced from 2.5 e^- to 0.25 e^-. The plot on the right shows the same time reduction in hours (black), as well as the total time to perform the observation (red).

where p is the pixel pitch.[5,6] Frequencies higher than ξ_N are aliased, and appear as spatial frequencies below the Nyquist frequency in images. The transfer function of a diffraction limited incoherent optical system at a wavelength λ, with a circular aperture of diameter D and focal length f, has a spatial frequency cutoff ξ_c:

$$\xi_c = \frac{1}{\lambda\left(\frac{f}{D}\right)} = \frac{D}{f\lambda}. \tag{2}$$

We can therefore define Q as the ratio of detector sampling frequency to the diffraction cutoff of the optics:

$$Q \equiv \frac{\frac{1}{p}}{\frac{D}{f\lambda}} = \frac{f\lambda}{Dp} = \frac{2\xi_N}{\xi_c} = 2\frac{\text{resolution}_{\text{optics}}}{\text{resolution}_{\text{sampling}}}. \tag{3}$$

$Q = 2$ implies $\xi_c = \xi_N$, which is the Nyquist sampling rate.[6] We can then examine the definition of the Airy diameter:

$$d_{\text{Airy}} = 2.44\frac{f\lambda}{D} = 2.44\left(\frac{f\lambda}{Dp}\right)p = 2.44Qp. \tag{4}$$

Thus, for diffraction-limited Nyquist sampling (where $Q = 2$),

$$d_{\text{Airy}} = 2.44Qp = 4.88p, \tag{5}$$

we have demonstrated that the flagship instrument needs 4.88 pixels across the Airy diameter. Figure 5 shows the pixel pitch required to achieve diffraction-limited Nyquist sampling at 500 nm across a range of f-numbers. We choose to present the data this way because the UV/O/IR mission planners and telescope designers will choose the final f-number to reduce the size and cost of the telescope, as well as aberration effects in the optical path. Lower f-numbers make the optical design more susceptible to spherical aberration, coma, and astigmatism, while greater f-numbers imply that the telescope must either be larger or contain multiple folds in the optical path. Since each fold requires reflection via a mirror, there is an associated loss of signal due to non-unity reflectivity.

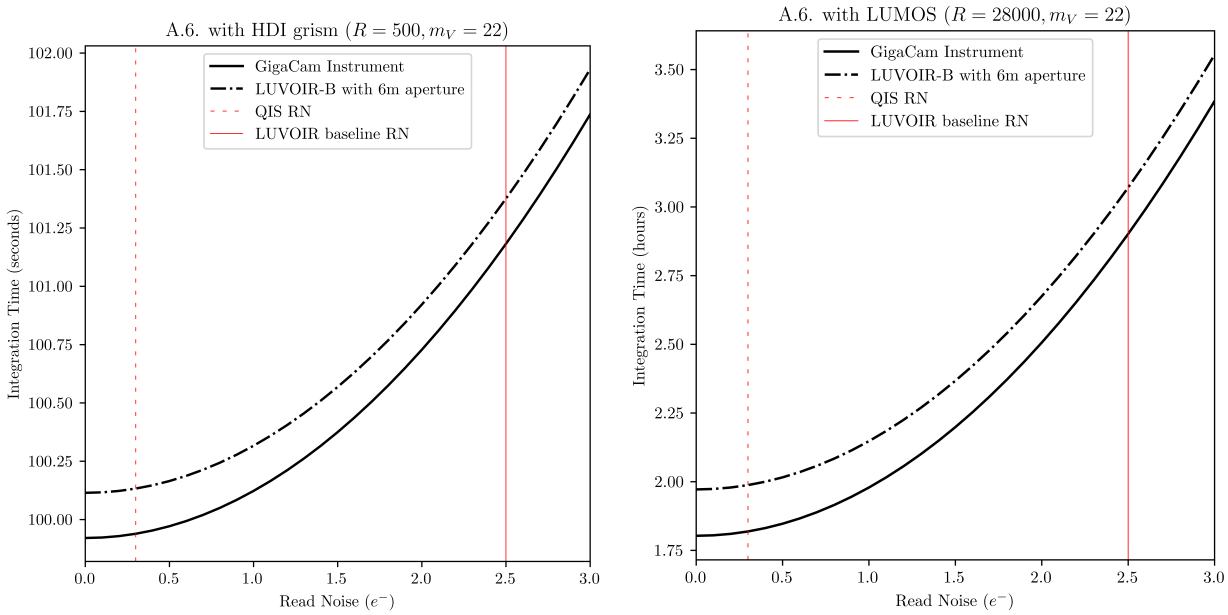

Figure 3. These plots show the total integration times to achieve SNR≥10 with low-medium resolution spectroscopy with HDI-B (R=500, left) and LUMOS (R=28000, right) for the 6 meter LUVOIR-B analog as a function of RN.

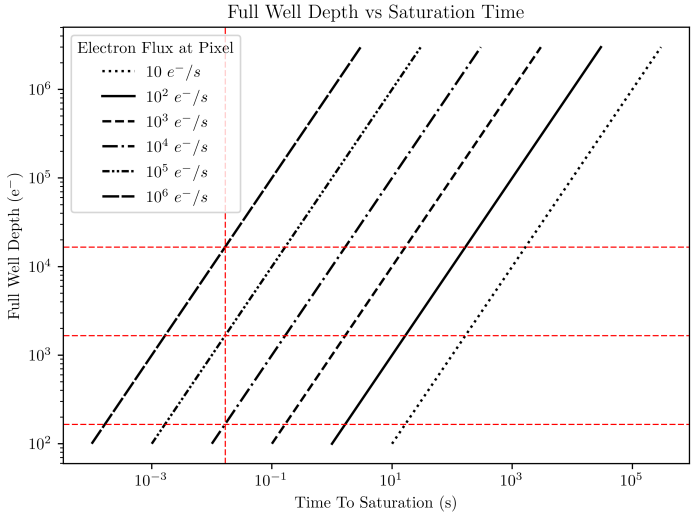

Figure 4. This plot shows the relationship between full-well depth and maximum integration time. The red lines mark the full well depth required to achieve 60 FPS readout without saturating the pixels.

4. COMPARING EXTANT TECHNOLOGIES

Two decades ago, CCDs almost completely dominated the field of astronomical detectors. CMOS detectors did not achieve performance better than CCDs by most performance metrics until the start of the 21st century, and have since surpassed them in most ways (this can be primarily attributed to advances in micro-electronic engineering.)[7] As one might expect, there has been significant effort to improve on the original CCD design since 1969, perhaps most notably with the invention of the Electron-Multiplying CCD (EMCCD). For the next generation of UV/O/IR observatories, the most promising technologies are photon-counting CMOS detectors, EMCCDs, Microwave Kinetic Inductance Detectors (MKIDs) and Superconducting Nanowire Single Photon

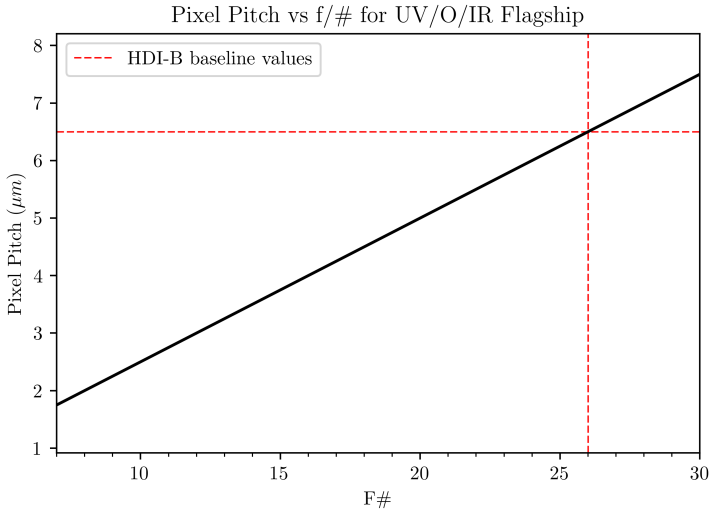

Figure 5. Pixel pitch as a function of f/# to maintain diffraction-limited Nyquist sampling. The red lines are the parameters baselined by the LUVOIR final report (f/26 and 6.5 μm pixel pitch).

Detectors (SNSPDs).

CCD and CMOS devices are the most popular choice of detector for astronomy, primarily due to the relatively low cost and ease of use. They have low power consumption, don't require cumbersome readout electronics, and don't require cooling to sub-Kelvin temperatures to achieve nominal performance characteristics (generally speaking, CMOS devices for astronomy are cooled to temperatures between 140-200 Kelvin, though some of the most recent detector chips are able to provide photon counting capability at room temperature.[8]) As the technology matures and micro-electronic processes improve, development teams have continued to advance the ability of these devices to provide observations with high SNR.

4.1 Maximizing SNR

All detector development is fundamentally driven by the desire to create the "ideal" device, one that is completely noiseless. In most CCDs and CMOS devices this means removing the dark current and RN. This is done to maximize the SNR, which is defined as

$$\mathrm{SNR} = \frac{\gamma \times \eta \times t}{\sqrt{\gamma \times \eta \times t + i_{\mathrm{dark}} \times t + RN^2}} \tag{6}$$

for a single pixel, where γ is the number of photons incident on the pixel, η is the quantum efficiency (the proportion of incident photons that are converted to photoelectric charge), t is the integration time, i_{dark} is the dark current, and RN is the electronic noise associated with reading out the pixel. Reducing the RN is complex, and is generally done using processes that involve multiple sampling (like the QIS technology) or signal multiplication (EMCCDs, LMAPDs, GMAPDs). Dark current, however, can be reduced down to a nominal noise floor simply by cooling the device chip. Since dark current is primarily a thermal effect causing electrons to be thermally excited out of the silicon lattice, a colder medium usually implies lesser dark current. Generally these devices are cooled to below 200 Kelvin, though some modern devices are able to achieve sub-electron RN at room temperature.[8,9] MKIDs are unique in comparison to CCD/CMOS technology in that they do not generate dark current of any kind - each photon generates an independent signal (thermal electrons lack the energy required to generate Cooper pairs, which are the primary signal generator in MKIDs.)[10]

In addition to reducing the noise, many recent developments aim to amplify the signal generated by the receiving pixel. EMCCDs do this by accelerating photoelectrons through a series of multiplication registers that each have a small probability ($\sim 2\%$) of generating a second electron by avalanche multiplication.[11] With a few

hundred multiplication stages, an overall gain of up to a few thousand is achievable. With a gain this high, the RN is reduced to negligible levels, and can be effectively removed from the SNR equation above. However, the process of electron multiplication introduces an Excess Noise Factor (ENF). ENF is introduced by statistical variation in the overall number of electrons created from an initial charge packet by the multiplication process. Effectively, this is a small probability that each step of transfer along the gain register produces an extra electron. ENF for EMCCDs has been evaluated at $\sqrt{2}$, and changes the SNR equation:

$$\mathrm{SNR} = \frac{G \times \gamma \times \eta \times t}{\sqrt{G \times \mathrm{ENF}^2 \times (\gamma \times \eta \times t + i_{\mathrm{dark}} \times t)}}, \tag{7}$$

where G is the gain factor.[11]

Photon-counting CMOS devices like the QIS have a very small capacitance at the floating diffusion sense node to create a large voltage response from a single electron without the need for avalanche gain. A single electron generates a signal significantly stronger than the typical voltage noise associated with the readout electronics. The voltage signal generated by a single photoelectron is

$$V = \frac{Q_e}{C_{\mathrm{FD}}}, \tag{8}$$

where Q_e is the charge of an electron and C_{FD} is the capacitance of the floating-diffusion node. The voltage response to a single electron is typically on the order of a few hundred microvolts for QIS.[9,12] This high conversion gain and low RN allows photon-counting CMOS devices to produce photon-counting histograms (PCH) with low bit error rate. Figure 6 is one such PCH for one of Gigajot's QIS cameras operating at 283 Kelvin.

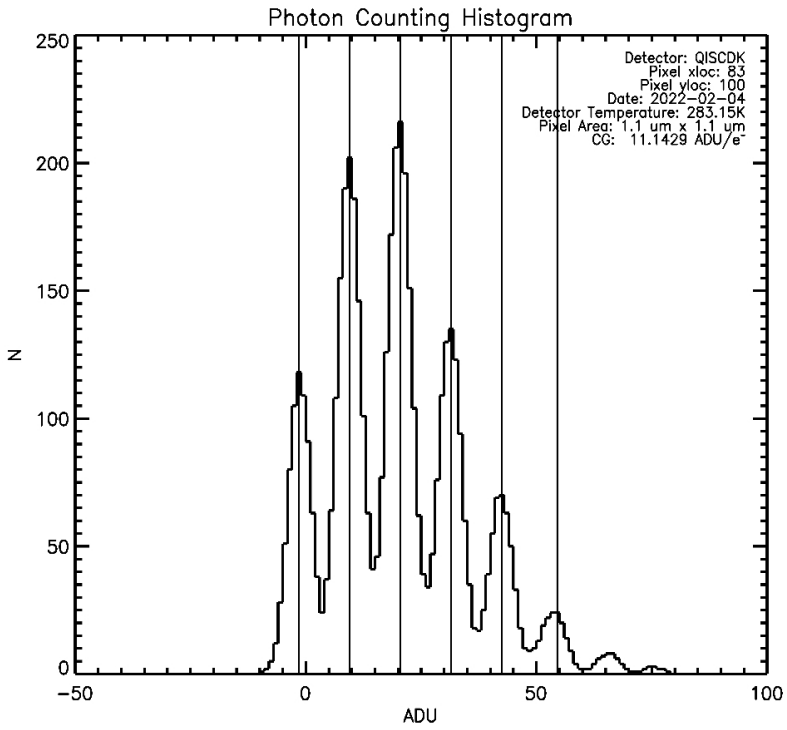

Figure 6. A photon counting histogram of a single pixel (5000 samples) taken with the commercial QIS camera development kit. The peaks represent no photons, 1 photon, 2 photons, 3 photons, and so forth. Note the high detector temperature of 283 Kelvin. This pixel has a read noise of 0.21 e^- and a conversion gain of 11.14 ADU/e^-, placing it in the top 35% of pixels on this detector.

4.2 Photon Energy Resolution

As silicon band-gap detectors, optical CMOS and CCD devices tend to produce only a single electron when a photon interacts with the detective bulk. This intrinsically limits the photon energy resolving ability of these devices to photon energies that are significantly higher than the band-gap energy.[10] For this reason, it is not common to see CMOS and CCD devices used in an energy-resolving capacity outside of deep-depletion devices for soft x-ray astronomy. There are superconducting devices that are intrinsically more capable of discerning the energy of incident photons directly, such as MKIDs, SNSPDs, and transition edge sensors (TES). MKIDs are the most promising of these technologies for UV/O/IR applications for a few reasons: they don't generate dark current, each pixel can act as a low to medium resolution spectrometer, they offer high time resolution, and are thus far the only superconducting detector technology that has demonstrated scalability to mega-pixel formats.[10,13] The advantages of the MKID energy resolution are evident when considered in the context of a proper spectrograph using a CMOS/CCD camera. For one, they eliminate the need for bulky refractive optics, and are thus much more compact - a high-resolution CCD spectrograph would require a large detector chip to allow for the dispersion of light spectra onto the detector face. High resolution multi-object spectrographs (HRMOS) have been suggested that would allow for high-resolution spectra of 100 objects simultaneously by utilizing fiber optic cables to direct light to multiple strips of MKID pixels.[13]

4.3 Scalability to Large Formats

One of the most important features of modern detectors that will be considered for the UV/O/IR flagship is scalability to mega- and giga-pixel formats. Detectors that can achieve high fill factor, large format focal plane arrays (FPA) are essential in order to utilize the full capabilities of a flagship-class observatory. Scaling to large formats carries a variety of challenges: ensuring adequate readout paths while maintaining buttability of FPA components, maintaining high fill-factor, ensuring power supply paths, thermal control of the FPA, and managing data output volume.[14]

CCD and CMOS devices are now commonly found in mega-pixel formats of 4K×4K pixels or more. EMCCDs have been fabricated and characterized at this size.[15] Photon-counting CMOS devices are commercially available in large formats from vendors such as Gigajot, Teledyne, and Hamamatsu. The team at the Center for Detectors at RIT has a 16 megapixel device from Gigajot, who recently created a 41 megapixel chip with 2 μm pixels. Gigapixel-format CMOS detectors like the one baselined for the GigaCam instrument have been proposed, and are a prime candidate for funding and development by the GOMTMP. Gigapixel CMOS has the advantage of simplifying the readout chain over an array of smaller detectors, while also having unity fill-factor. However, there are challenges with production yield for the large wafers that would be required to create such a device, even with pixels of 1-2 μm size. EMCCDs present a larger challenge when scaling to a single giga-pixel array (CTE, susceptibility to radiation damage, clock-induced-charge) somewhat lessening the benefit of scaling to a single gigapixel array in comparison to a CMOS architecture. Some of these issues are mitigated in segmented CCD designs.

MKIDs have been demonstrated in arrays as large as 20,440 pixels, but do not currently exist in mega-pixel formats. MKIDs also currently require large readout electronic stacks, despite being one of the easiest detector technologies to multiplex.[10,16] There are, however, ongoing efforts to reduce the size of these electronics and make them more efficient.[17] SNSPDs - while especially promising for UV astronomy - currently do not have readout architectures to support mega-pixel format arrays. The largest SNSPD readout architectures have only been able to support arrays on the order of a kilo-pixel, and are unlikely to be scaled to tens of kilo-pixels. There is work to underway to create a robust, scalable architecture for mega-pixel SNSPD arrays, but has only been demonstrated thus far using a proof-of-concept kilo-pixel device.[18]

5. CONCLUSIONS

We have discussed the science goals from the LUVOIR Final Report that provide the most stringent requirements on detectors for the next great observatory. The two extremes (observations of very bright and dim objects) place important constraints on the full-well depth, readout speed, read noise, and dark current that the devices must deliver in order to be considered for the mission. Pixel size is entirely dependent on the architecture of the instrument and observatory; the trades that have to be made between pixel pitch, FWD, RN, and dark current

should be carefully considered and presented prior to the final decisions on the architecture of the UV/O/IR flagship.

Many existing detector technologies are able to deliver DC/RN performance well below the required level to perform the science required of the next great observatory. Photon-counting CMOS detectors are being rapidly developed to large formats with high FWD, fast readout, and improved uniformity. EMCCDs have much better RN performance due to their gain mechanism, and are rapidly improving how they deal with CIC and cosmic ray impacts.[15] MKIDs are becoming more viable as the technology matures, but still require resource-expensive technologies to perform device readout and maintain superconducting temperatures, making them somewhat undesirable for space missions despite their otherwise incredible performance. SNSPDs are promising for UV astronomy, but suffer from some of the same issues as MKIDs in regard to refrigeration and readout architecture.

ACKNOWLEDGMENTS

The team at the Center for Detectors would like to acknowledge Bob Woodruff for creating the GigaCam instrument design and providing the ray-traces. This work was supported by the NASA Cosmic Origins (COR) program office under the Strategic Astrophysics Technology (SAT) program Grant No. 80NSSC20K0310.

REFERENCES

[1] National Academies of Sciences, E. and Medicine, [*Pathways to Discovery in Astronomy and Astrophysics for the 2020s*], The National Academies Press, Washington, DC (2021).

[2] The LUVOIR Team, "The LUVOIR Mission Concept Study Final Report Appendices," (Aug. 2019).

[3] The LUVOIR Team, "The LUVOIR Mission Concept Study Final Report," *arXiv e-prints* , arXiv:1912.06219 (Dec. 2019).

[4] Gallagher, J. P., Buntic, L., and Figer, D. F., "Characterization of single-photon sensing and photon-number resolving cmos image sensors," *Proc. of SPIE* **12191** (In Press).

[5] Janesick, J. R., [*Scientific charge-coupled devices*] (2001).

[6] Fiete, R. and of Photo-optical Instrumentation Engineers, S., [*Modeling the Imaging Chain of Digital Cameras*], SPIE Digital Library, Society of Photo Optical (2010).

[7] Fowler, B., Liu, X., and Vu, P., "Cmos image sensors-past present and future," *Society for Imaging Science and Technology* (2006).

[8] Ma, J. and Fossum, E. R., "Quanta Image Sensor Jot With Sub 0.3e- r.m.s. Read Noise and Photon Counting Capability," *IEEE Electron Device Letters* **36**, 926–928 (Sept. 2015).

[9] Ma, J., Masoodian, S., Starkey, D. A., and Fossum, E. R., "Photon-number-resolving megapixel image sensor at room temperature without avalanche gain," *Optica* **4**, 1474 (Dec. 2017).

[10] Ulbricht, G., Lucia, M. D., and Baldwin, E., "Applications for microwave kinetic induction detectors in advanced instrumentation," *Appl. Sci.* **11** (2021).

[11] Djazovski, O., Daigle, O., Laurin, D., Bedirian, M., and Ducharme, M., "Electron-multiplying ccds for future space instruments," in [*Photonics North*], *Proc. SPIE* **8915** (2013).

[12] Deng, W. and Fossum, E. R., "1/f Noise Modelling and Characterization for CMOS Quanta Image Sensors," *Sensors* **19**, 5459 (Dec. 2019).

[13] Mazin, B., Bailey, J., Bartlett, J., Bockstiegel, C., Bumble, B., Coiffard, G., Currie, T., Daal, M., Davis, K., Dodkins, R., Fruitwala, N., Jovanovic, N., Lipartito, I., Lozi, J., Males, J., Mawet, D., Meeker, S., O'Brien, K., Rich, M., Smith, J., Steiger, S., Swimmer, N., Walter, A., Zobrist, N., and Zmuidzinas, J., "MKIDs in the 2020s," in [*Bulletin of the American Astronomical Society*], **51**, 17 (Sept. 2019).

[14] Scowen, P., Nikzad, S., Hoenk, M., Gontijo, I., Shapiro, A., Greer, F., Jones, T., Seshadri, S., Jacquot, B., Monacos, S., Lisman, D., Dicki, M., and Blacksberg, J., "Large Focal Plane Arrays for Future Missions," in [*astro2010: The Astronomy and Astrophysics Decadal Survey*], **2010**, 30 (Mar. 2009).

[15] Daigle, O., Turcotte, J., Artigau, É., and Doyon, R., "Preliminary characterization results of a large format 4k × 4k EMCCD," in [*High Energy, Optical, and Infrared Detectors for Astronomy VIII*], Holland, A. D. and Beletic, J., eds., *Society of Photo-Optical Instrumentation Engineers (SPIE) Conference Series* **10709**, 107090A (July 2018).

[16] Meeker, S. R., Mazin, B. A., Walter, A. B., Strader, P., Fruitwala, N., Bockstiegel, C., Szypryt, P., Ulbricht, G., Coiffard, G., Bumble, B., Cancelo, G., Zmuda, T., Treptow, K., Wilcer, N., Collura, G., Dodkins, R., Lipartito, I., Zobrist, N., Bottom, M., Shelton, J. C., Mawet, D., van Eyken, J. C., Vasisht, G., and Serabyn, E., "Darkness: A microwave kinetic inductance detector integral field spectrograph for high-contrast astronomy," *Publications of the Astronomical Society of the Pacific* **130**, 065001 (June 2018).

[17] Fruitwala, N., Strader, P., Cancelo, G., Zmuda, T., Treptow, K., Wilcer, N., Stoughton, C., Walter, A. B., Zobrist, N., Collura, G., Lipartito, I., Bailey, J. I., and Mazin, B. A., "Second generation readout for large format photon counting microwave kinetic inductance detectors," *Review of Scientific Instruments* **91**, 124705 (Dec. 2020).

[18] McCaughan, A. N., Zhai, Y., Korzh, B., Allmaras, J. P., Oripov, B. G., Shaw, M. D., and Nam, S. W., "The thermally-coupled imager: A scalable readout architecture for superconducting nanowire single photon detectors," *arXiv e-prints* , arXiv:2112.04705 (Dec. 2021).